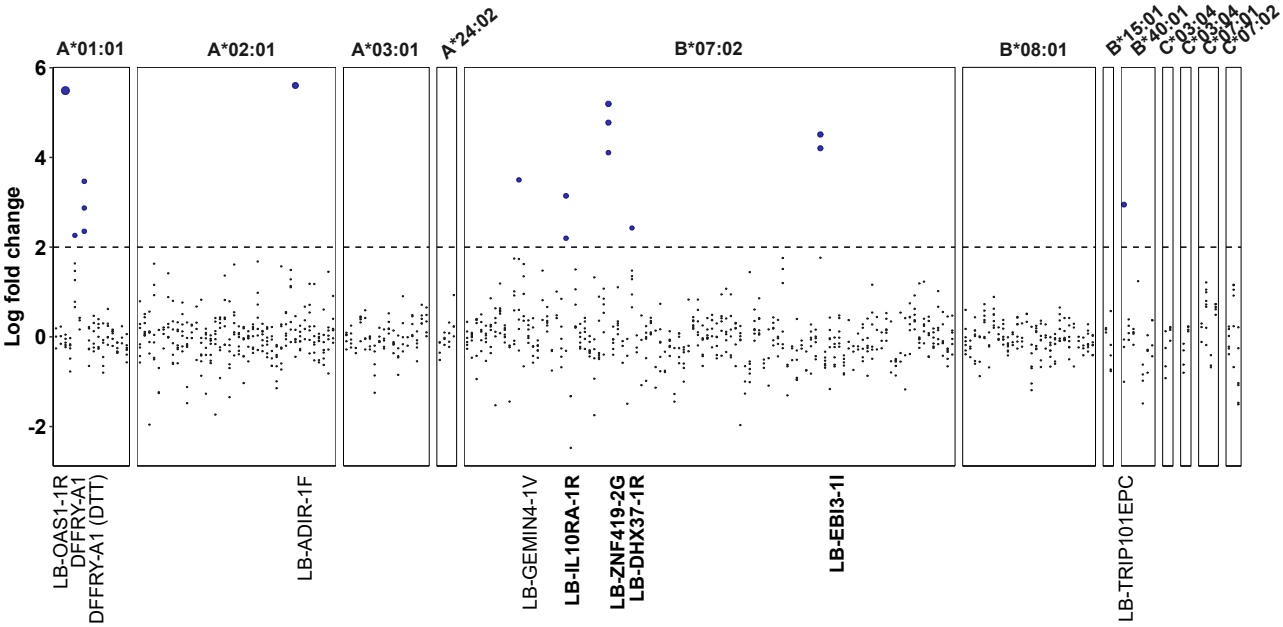

Supplemental Figure 1. Staining of healthy donor samples with pMHC-multimers. To investigate potential background staining of pMHC-multimers, all pMHC-multimer mixes were used to stain pools of healthy third-party donors containing at least one donor expressing the HLAs of interest. For 10 pMHC-multimers, T cells were measured (blue). Four of these pMHC-multimers (bold font) were also detected in 4-7 patients who were not mismatched for the MiHAs, and therefore excluded from further analysis. This included the untreated LB-DHX37-1R peptide, whereas pMHC-multimers with cysteinylated or reduced peptide variants of LB-DHX37-1R did not show any background staining and remained included in the analysis.

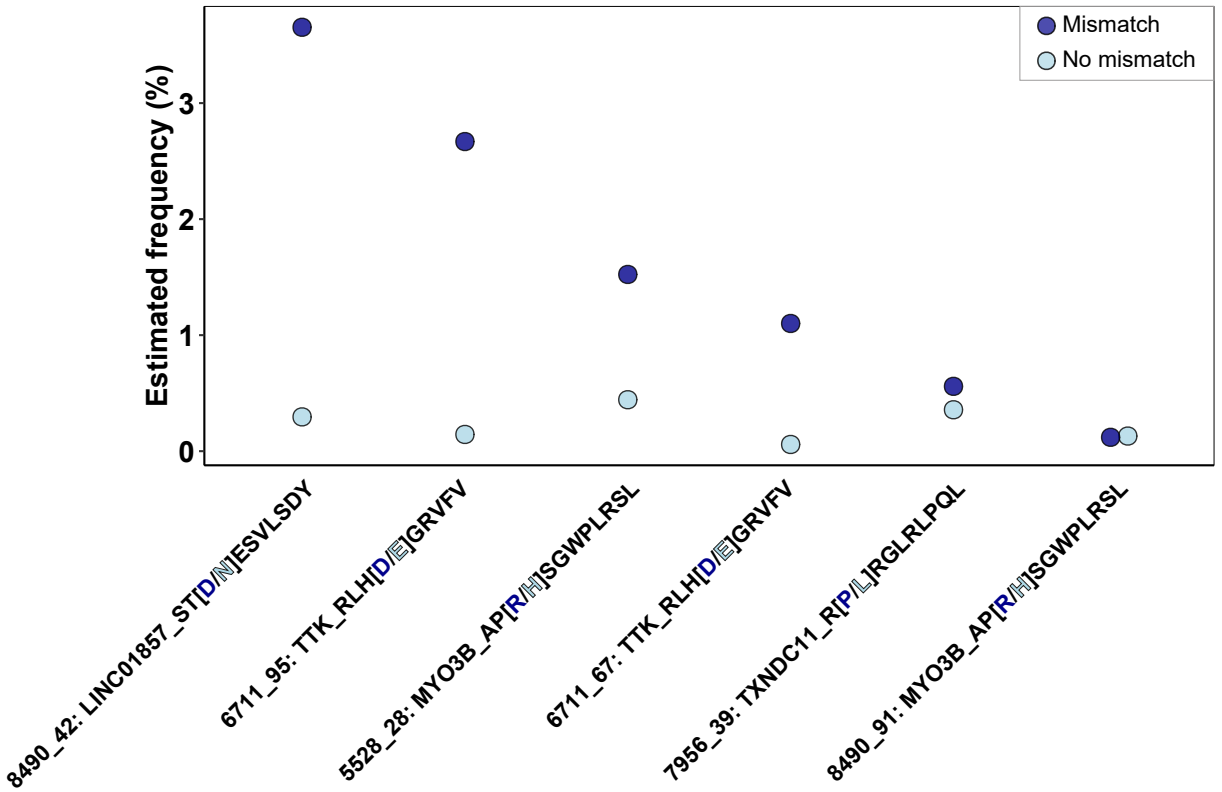

Supplemental Figure 2. T-cell frequencies for MiHAs and allelic variants in the same samples. In six samples, T cells were detected for both MiHAs and their allelic variants. Patients were mismatched (dark blue) or not mismatched (light blue) for the respective variant. Labels indicate the patient number, timepoint of the sample (days after DLI), MiHA-encoding gene, and peptide sequence [mismatched/non-mismatched amino acid].

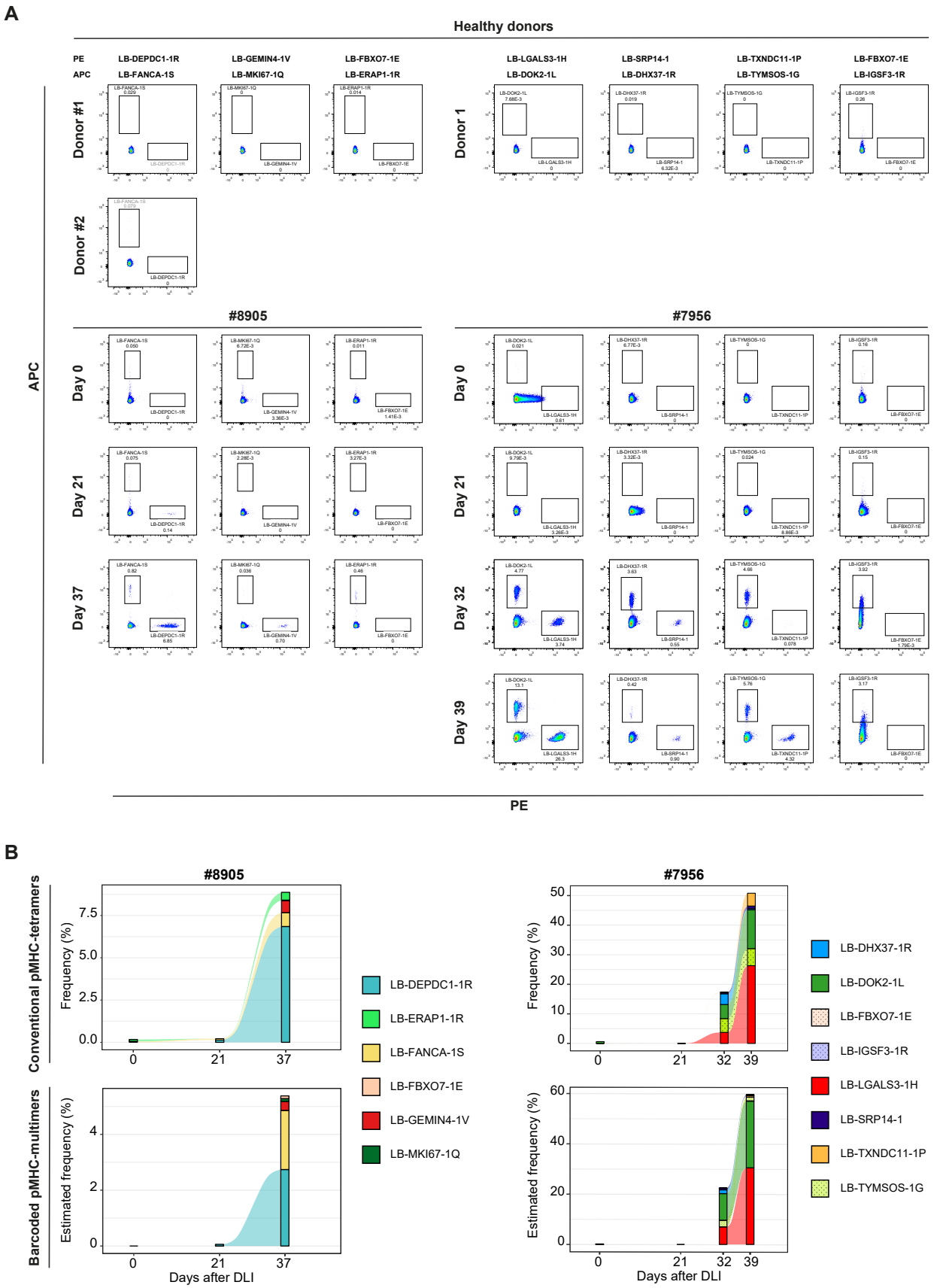
A
Healthy donors
PE
APC
LB-DEPDC1-1R
LB-FANCA-1S
LB-GEMIN4-1V
LB-MKI67-1Q
LB-FBXO7-1E
LB-ERAP1-1R
LB-LGALS3-1H
LB-DOK2-1L
LB-SRP14-1
LB-DHX37-1R
LB-TXNDC11-1P
LB-TYMSOS-1G
LB-IGSF3-1R
Donor #1
Donor #2
Donor 1
#8905
#7956
Day 0
Day 21
Day 32
Day 37
Day 39
PE
B
Conventional pMHC-tetramers
Barcoded pMHC-multimers
Frequency (%)
Estimated frequency (%)
Days after DLI
LB-DEPDC1-1R
LB-ERAP1-1R
LB-FANCA-1S
LB-FBXO7-1E
LB-GEMIN4-1V
LB-MKI67-1Q
LB-DHX37-1R
LB-DOK2-1L
LB-FBXO7-1E
LB-IGSF3-1R
LB-LGALS3-1H
LB-SRP14-1
LB-TXNDC11-1P
LB-TYMSOS-1G

Supplemental Figure 3. T-cell frequencies for MiHAs by conventional fluorescent pMHC-tetramers. For patients #8905 and #7956, MiHA-specific T-cell responses detected by barcoded pMHC-multimers were validated by conventional fluorescent pMHC-tetramers. (**A**) PE- or APC-conjugated conventional fluorescent pMHC-tetramers were produced for 13 MiHAs. T cells for these MiHAs were detected by barcoded pMHC-multimers in patients #8905 and #7956 for all MiHAs, except for LB-ERAP1-1R. We previously isolated a T-cell clone for LB-ERAP1-1R from patient #8905, and therefore included the MiHA in the panel of conventional pMHC-tetramers. Conventional pMHC-tetramer staining for 12 MiHAs binding to HLA-B*07:02 was performed for potential background staining on PBMCs from an HLA-B*07:02-positive donor (donor #1). The PE-conjugated pMHC-tetramer for LB-DEPDC1-1R, which binds to HLA-B*08:01, was tested for potential background staining on PBMCs from an HLA-B*08:01-positive donors (donor #2). All pMHC-tetramers showed no or low background staining, except for the APC-conjugated pMHC-tetramer for LB-IGSF3-1R. T cells detected with barcoded pMHC-multimers against mismatched MiHAs (LB-DEPDC1-1R, LB-FANCA-1S, LB-GEMIN4-1V and LB-MKI67-1Q in patient #8905; LB-DHX37-1R, LB-DOK2-1L, LB-LGALS3-1H, LB-SRP14-1 and LB-TXNDC11-1P in patient #7956) were all confirmed by conventional pMHC-tetramer staining. For patient #7956, T cells detected with barcoded pMHC-multimers against the non-mismatched antigen LB-TYMSOS-1G were also confirmed by pMHC-tetramers, but T-cell responses against the non-mismatched antigen LB-FBXO7-1E in both patients were not confirmed. Conventional tetramer staining for the non-mismatched LB-IGSF3-1R in patient #7956 was low in mean fluorescence intensity and may have been caused by non-specific background staining as indicated by staining of healthy donor PBMCs. (**B**) Longitudinal screening of patients #8905 and #7956 by fluorescent pMHC-tetramers (top panel) and barcoded pMHC-multimers (bottom panel) revealed induction of immune responses against MiHAs with similar kinetics.

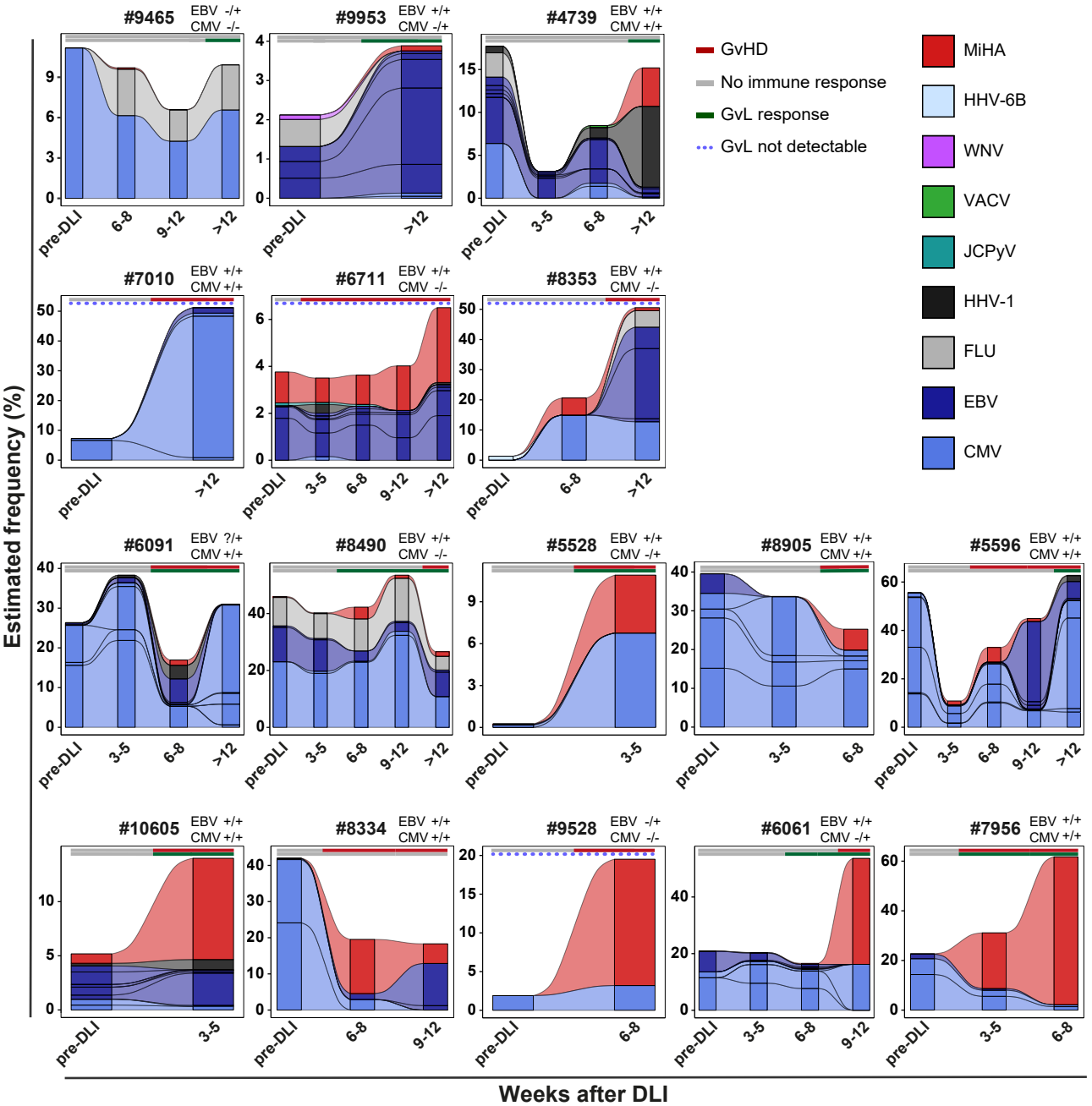

Supplemental Figure 4. T-cell frequencies against viral antigens and MiHAs in patients responding to DLI after HLA-matched alloSCT. Indicated are estimated T-cell frequencies by barcoded pMHC-multimers for viral antigens and MiHAs in patients responding to DLI after HLA-matched alloSCT. Of the 16 patients, three patients responded to DLI without GvHD (patients #9465, #9953, #4739), three patients developed limited GvHD (patients #7010, #6711, #8353) and 10 patients had severe GvHD (#6091, #8490, #5528, #8905, #5596, #10605, #8334, #9528, #6061, #7956). Indicated is the EBV (Epstein Barr virus) and CMV (cytomegalovirus) serostatus for all patients and donors prior to alloSCT (patient/donor), except for patient #6091 whose serostatus for EBV is unknown. All patients showed high T-cell frequencies for EBV and/or CMV. A few patients had low T-cell frequencies against human herpesvirus type 6B (HHV-6B), West Nile virus (WNV), vaccinia virus (VACV), human polyomavirus (JCPyV), human herpesvirus type 1 (HHV-1) or influenza virus (FLU) peptides.

Supplemental Figure 5

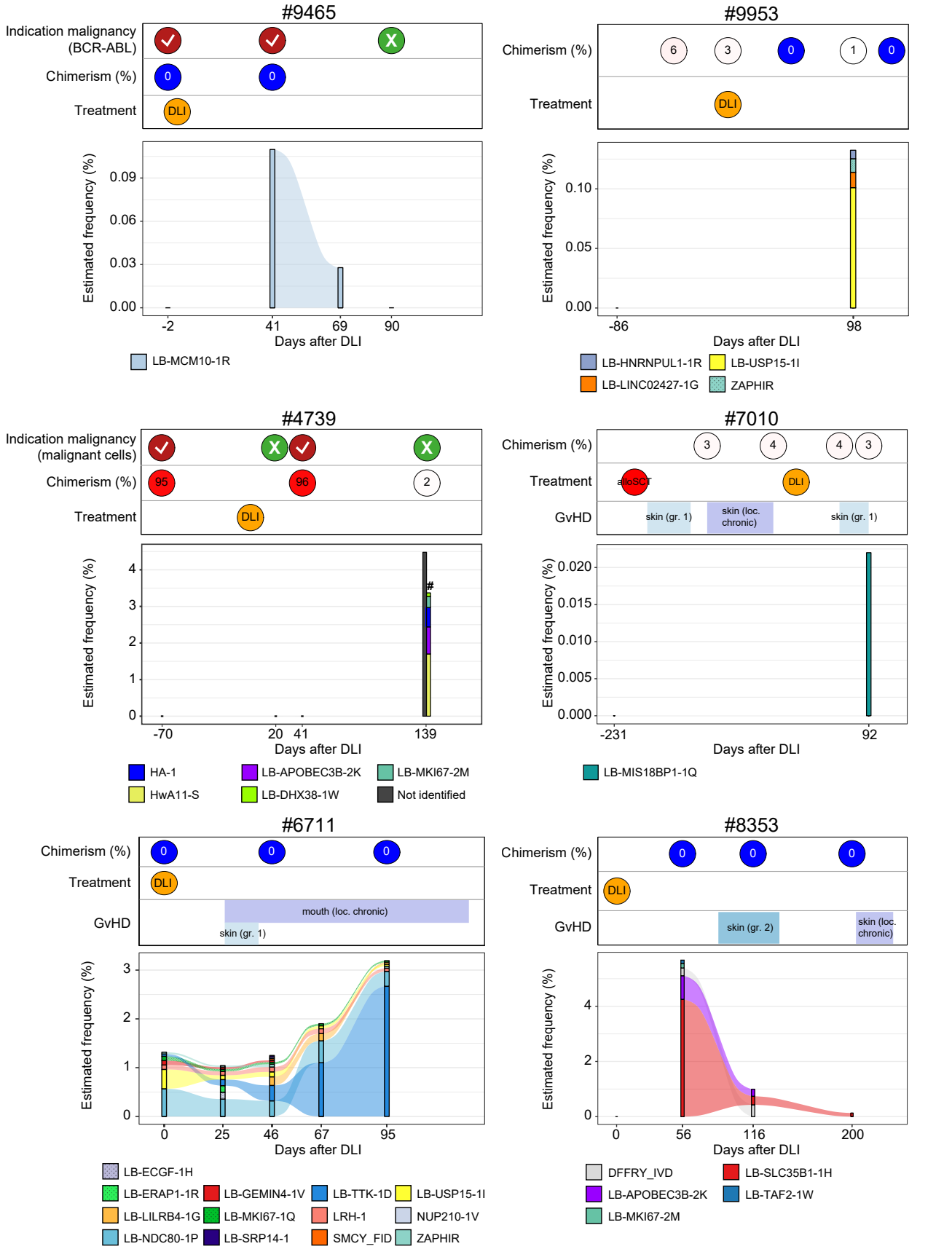

Supplemental Figure 3

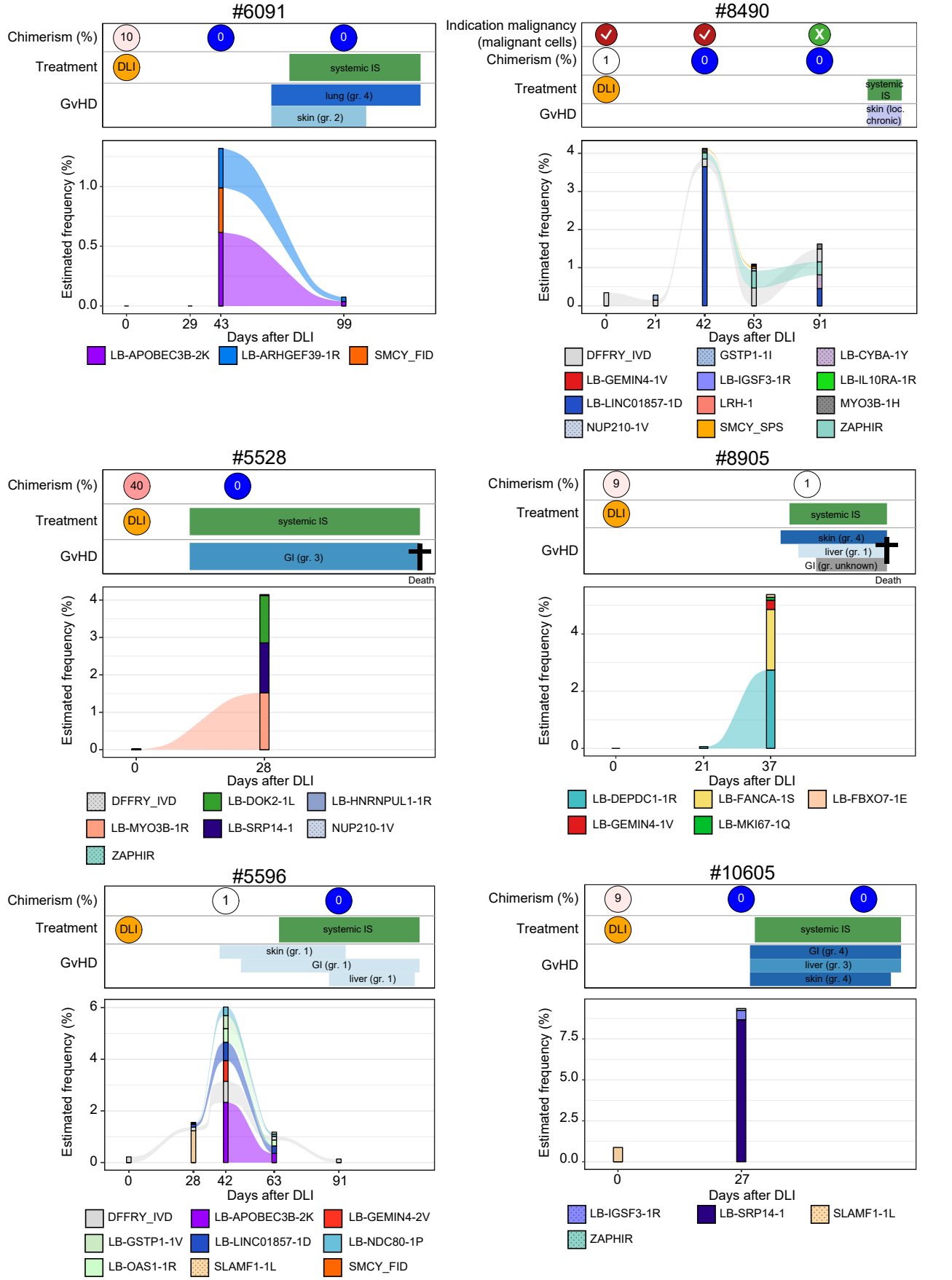

Supplemental Figure 5 (continued)

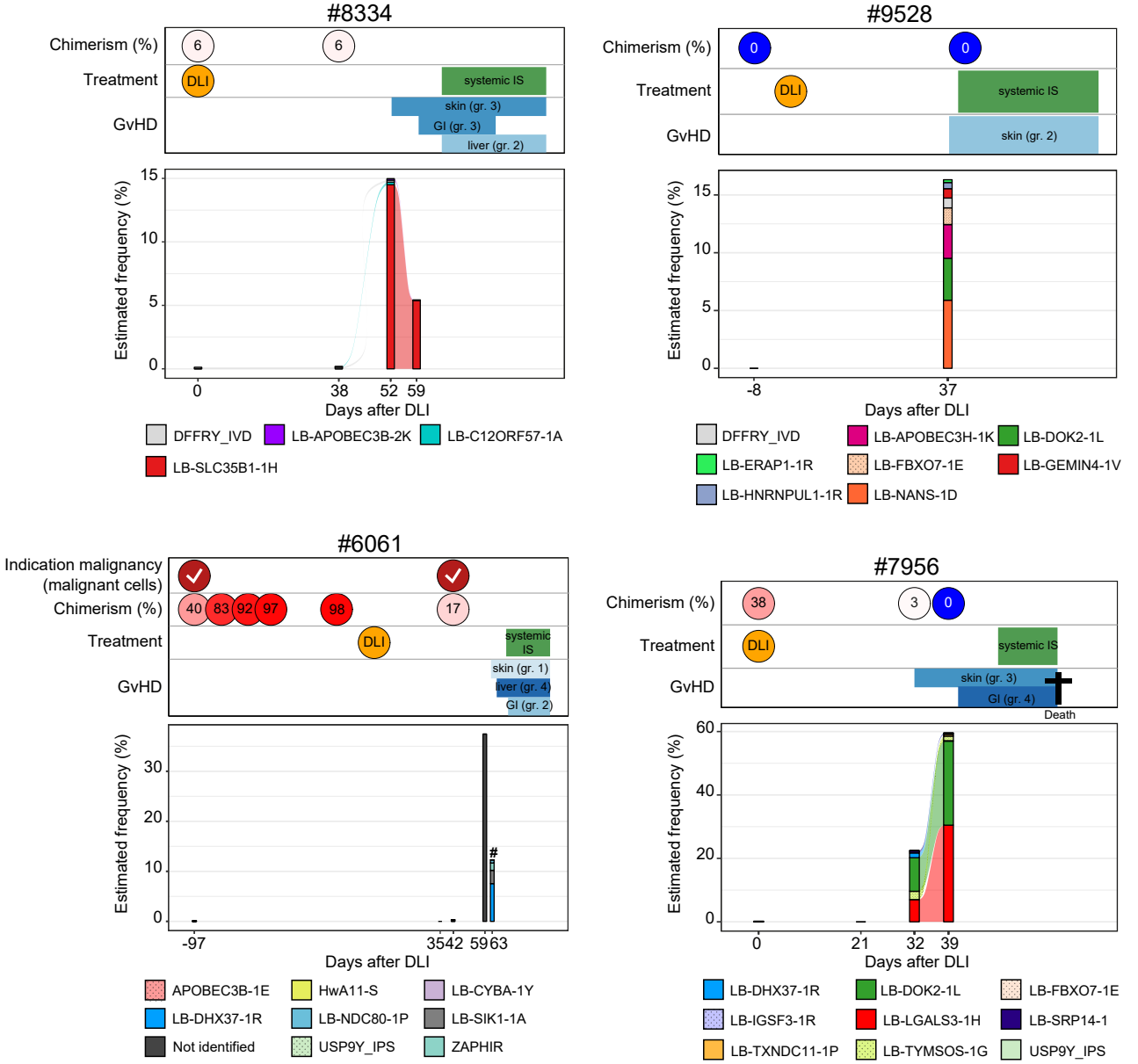

Supplemental Figure 5. Frequencies of MiHA-specific T cells in patients during development of GvL and GvHD. T-cell frequencies for individual MiHAs are shown for 16 patients during development of GvL and GvHD after DLI. After DLI, patients experienced an immune response in the form of GvHD or disappearance of hematopoietic patient cells. This is indicated, if applicable, by conversion to full-donor chimerism or disappearance of malignant cells based on detection of tumor-specific markers by qPCR (BCR-ABL) or flow cytometry. Information on GvHD or treatment with systemic immunosuppressive agents is indicated if patients developed GvHD or received immunosuppressive agents. Information on tumor markers dependent on the underlying disease is indicated if patients were positive for measurable residual disease during treatment with DLI. Dotted colors indicate T-cell measurements against MiHAs in patients who were not mismatched for these antigens. Hashtags indicate two samples for which T-cell frequencies were measured by conventional fluorescent pMHC-tetramer staining.